ACS Sustainable Resource Management

pubs.acs.org/acssrm

Article

Investigation of the Thermal and Mechanical Properties of Hydrolyzed-Collagen-Reinforced Poly(lactic acid) Composite Blown Films

Radhika Panickar and Vijay K. Rangari*

Cite This: https://doi.org/10.1021/acssusresmgt.4c00282

Read Online

ACCESS | Metrics & More | Article Recommendations | Supporting Information

ABSTRACT: Poly(lactic acid) (PLA) is a biodegradable polyester polymer that is a promising material for replacing petroleum-based polymers in various applications. The present study investigates the mechanical and thermal properties of hydrolyzed collagen (HC) powder-reinforced biopolymer composite blown films. The biodegradable polymer PLA was reinforced with HC at different weight percentages (0.5%, 0.75%, 1%, and 1.25%) using the solution blending method in chloroform, followed by blown-film extrusion. Among different weight percentages of HC in the PLA matrix, 1 wt % HC reinforced with PLA blown films exhibited significant changes and improvements in the FTIR, XRD, TGA, and DSC analyses. A polymer blend formation from PLA and 1% HC was observed in XRD, FTIR, and Raman analyses, exhibiting chemical bonding of the amide group to the PLA backbone. It was understood that intermolecular interaction of the PLA and HC molecules was due to the inter-H bonds of the −NH, −OH, and −CH functional groups. The thermal behavior and crystallinity of the PLA/HC composite films were investigated using TGA and DSC. Compared with other film samples, PLA/1% HC exhibited a higher thermal stability of 360.29 °C. The tensile studies show significant enhancement in the flexibility with a high elongation strength of PLA/HC composite films compared to neat PLA films. The fracture analysis of PLA/1% HC confirms the interfacial compatibility and transformation to plastic deformation due to the chemical bonding of HC in the PLA matrix. The PLA/HC composite films exhibit UV barrier properties that are recommended for food packing applications.

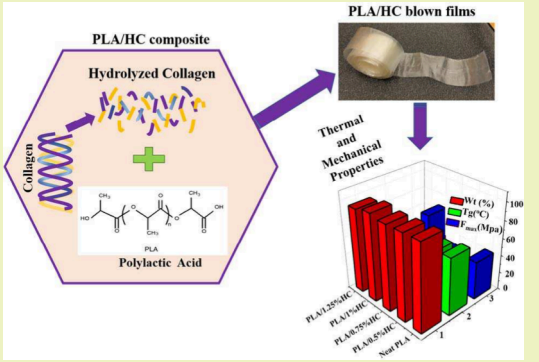

KEYWORDS: *biodegradable polymer, polymer composites, poly(lactic acid), hydrolyzed collagen, food packaging*

1. INTRODUCTION

Recently, the continuous consumption of plastic products,[1−3] the future scarcity of petroleum resources,[4,5] and the increasing threat of plastic waste have led to the development and research of non-petroleum-based biodegradable polymer materials.[6−8] In the past decade, many biobased and biodegradable polymers have been introduced in the market, among which poly(lactic acid) (PLA) is a biodegradable polyester that is widely researched and developed.[9,10] This compostable and versatile polymer is a linear aliphatic thermoplastic polyester synthesized from the fermentation of renewable resources, such as sugar beet and corn starch. During PLA production, it consumes a low amount of energy and produces minimum greenhouse gases. PLA has excellent properties such as biocompatibility, biodegradability, transparency, high strength, and modulus. Besides, they are easily processed using conventional thermoplastic processing techniques such as thermoforming, injection molding, blown film, and filament extrusions.[11,12]

As a biodegradable polymer, PLA is generally recognized as safe (GRAS) for food contact surfaces. However, their drawbacks are relatively low gas barrier (O_2 and water vapor) properties, low thermal stability, and brittleness, which limits the use of PLA in food-packaging applications.[13,14] Numerous studies have been reported on multiple procedures to overcome these disadvantages of PLA by chemical modification, nucleation, block copolymerization, plasticizers, and blending with suitable polymers.[15−17] The chemical routes and copolymerization methods are complex and typically expensive, affecting production costs. Blending with suitable polymers is another way to enhance polymers' mechanical and physical properties. However, blending can cause negative impacts such as chemical interaction, low tensile strength and modulus, and degradation properties in PLA.[18]

Another method is adding organic or inorganic fillers in polymers that can act as nucleating agents to improve

Received: July 19, 2024
Revised: December 4, 2024
Accepted: December 4, 2024

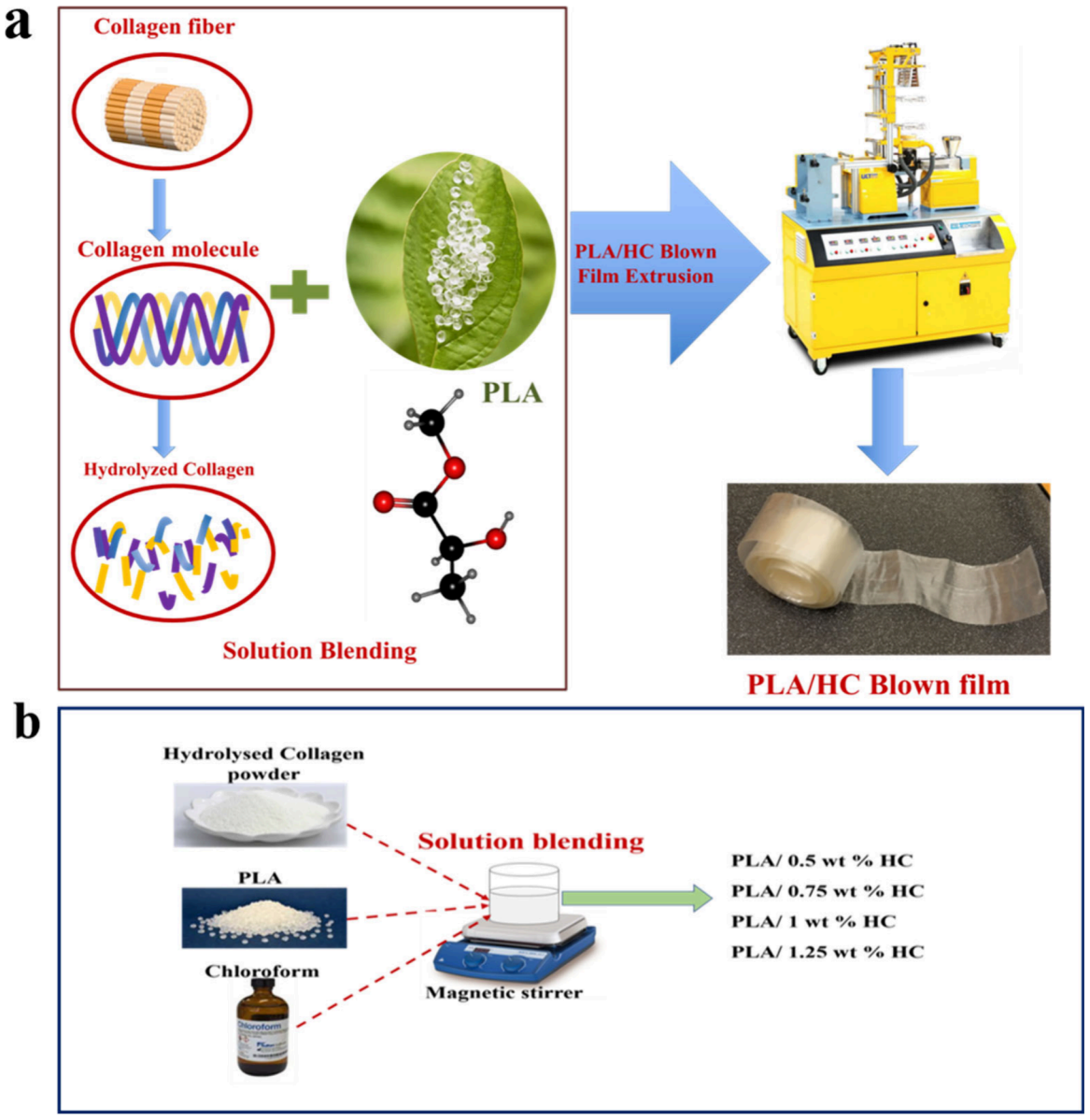

Figure 1. (a) Diagram illustrating the method of PLA/HC composite blown-film preparation using an ultramicrofilm blowing line type LUMF-150 single screw extruder. (b) Schematic representation of the different weight percentages of PLA/HC composite preparation using solution mixing.

polymers' flexibility, strength, toughness, thermal stability, and barrier properties, even when added at very low concentrations in a polymer.[19,20] Numerous investigations have been reported on the addition of natural and waste fillers that act as nucleating agents to reinforce the PLA backbone to achieve flexibility and crystallinity, such as natural fibers,[21] aluminum silicates,[22] hydroxyapatite,[23] calcium carbonate,[24] collagen,[25] etc. Moreover, by enhancement of the properties of the polymer composite, these natural fillers help to improve partial decomposition of the polymer, thereby partly solving environmental issues.

Among these natural fillers in polymers, collagen is a natural protein found in animal connective tissues that generally aids in strengthening skin elasticity and flexibility. Collagen as polymer filler exhibits interesting mechanical and biological properties and forms a good blend with natural polymers.[26] Collagen is made of three chains of amino acids wound together as helixes, as shown in Figure 1a. A hydrolysis process can break down these amino acids into small peptide molecules, forming hydrolyzed collagen (HC) with excellent solubility. Hydrolyzed collagen with small peptide molecules is extensively used as a dietary skin antiaging supplement that is easy for the body to absorb and digest.[27]

A few studies have been reported on PLA and collagen composites in various medical applications.[28−30] However, no studies have been reported on the detailed analysis of PLA and HC composites made from blown-film extrusion for potential food-packing applications. The main aim of this study is to investigate the effect of HC in the PLA matrix and its potential use in food-packaging applications. The thermal and mechanical properties of HC as a natural filler in the PLA matrix were thoroughly investigated. A detailed materials characterization of the HC and PLA/HC composite blown film was performed using X-ray diffraction (XRD), Fourier transform infrared (FTIR), Raman spectroscopy, scanning electron microscopy (SEM), thermogravimetric analysis (TGA), and differential scanning calorimetry (DSC). It was understood that HC compared to natural collagen gives

https://doi.org/10.1021/acssusresmgt.4c00282
ACS Sustainable Resour. Manage. XXXX, XXX, XXX−XXX

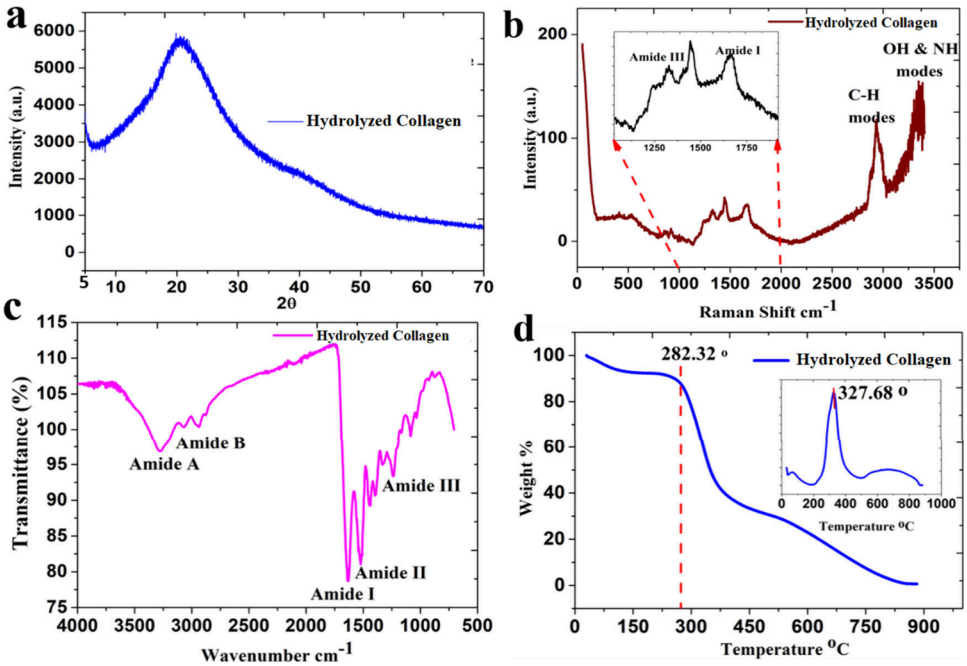

Figure 2. Characterization of hydrolyzed collagen powder: (a) XRD pattern; (b) Raman spectrum; (c) FTIR spectrum; (d) TGA.

excellent solubility and can blend more into the polymer matrix due to the small peptide molecules. The study reveals significant improvement in the thermal and mechanical properties of the biodegradable PLA/HC composite films for potential applications in food packaging.

2. EXPERIMENTAL SECTION

2.1. Materials. Commercially available consumable hydrolyzed collagen powder (Mama natural multicollagen powder) from the market was used to prepare PLA/HC composite blown films with Type I, II, III, IV, V, and X collagens. Poly(lactic acid) (PLA) pellets 4032D were purchased from Natureworks LLC, USA. Chloroform (≥99.8% with 0.5− 1% ethanol as a stabilizer) for dissolving PLA pellets was procured from Sigma-Aldrich (St. Louis, MO).

2.2. Preparation of the PLA/HC Composite. A simple solution blending method was used to prepare the PLA/HC composite, where chloroform was used as the solvent that can effectively dissolve PLA pellets. Hydrolyzed-collagen-reinforced PLA composites were prepared using different weight percentages of HC powder in PLA. Figure 1 b shows the schematic representation of the PLA/HC composite preparation with 0.5, 0.75, 1, and 1.25 wt % of HC in PLA. Different weight percentages of HC powder were stirred in 200 mL of chloroform for 30 min to disperse the HC, followed by continuously adding PLA pellets stirred at 600 rpm for 6 h at room temperature. The well-dispersed PLA/HC solutions were transferred to an aluminum tray to evaporate the solvent under a fume hood. The dried PLA/HC composite sheets were then chopped into small pieces for film extrusion.

2.3. Preparation of PLA/HC Composite Blown Films. All of the PLA/HC composite blown films (0.5, 0.75, 1.0, and 1.25 wt %) were produced using an ultramicrofilm blowing line type LUMF-150 single screw extruder by Lab Tech Engineering Company Ltd. (Figure 1a). The chopped biocomposite polymer with different weight percentages of HC in PLA was fed into the hopper with a screw speed maintained at 60 rpm. The screw assembly was a single conical screw with a diameter of 18 mm at the feed section and narrowing down to 8 mm at the screw end. It possesses an L/D ratio of 30:1. The melting temperature of the neat PLA polymer obtained from DSC analysis was set as the barrel temperature. The single screw blown film extruder has two heating zones that can be controlled independently. The barrel and die temperatures for the blown-film extrusion of PLA/HC composite were set at 170 °C (340 °F) and 163 °C (325 °F), respectively. The film die assembly had a 20 mm film die, and an air ring was provided to the blower to cool the exterior side of the blown film. The blower speed was kept between 900 and 1000 rpm to cool the blown films from the die assembly. Different weight percentages of PLA/HC composite films were extruded through the die and directed through the spring-loaded nip rolls to the winding bobbin at the other end of the machine to roll down the films. Figure 1a shows the blown film extruded for a 1 wt % HC/PLA composite.

2.4. Characterization Techniques. The HC was characterized by using a Rigaku Smartlab X-ray diffractometer equipped with monochromatic Cu $K\alpha_1$ radiation. The sample was scanned at a scan rate of 1°/min from 1° to 70° Bragg angle at 45 kV and 40 mA. A Thermo Scientific DXR Raman spectrometer with a 780 nm excitation wavelength was used for chemical analysis of the HC and PLA/HC composite films prepared at different weight percentages. The spectrum was analyzed from 0 to 3500 cm^{-1} with a laser power of 5 mW. The functional groups attached to the HC and PLA/HC composite films were analyzed using a FTIR spectrometer (IR Tracer-100) with a high resolution at 0.25 cm^{-1} and a high scanning speed. The structure and morphology of the hydrolyzed collagen powder and PLA/HC composite films were imaged using a JEOL JSM-7200F field-emission scanning electron microscope. Before imaging, all samples were gold-sputtered for 30 s using a sputter coater. The hydrolyzed collagen powder and the fracture analysis of the PLA/HC composite films were imaged at an accelerating voltage of 10 kV, and the surface of the PLA/HC composite films was imaged at an accelerating voltage of 5 kV.

2.5. Thermal Property Testing. The decomposition temperature and weight change of the HC and PLA/HC composite films were studied by using a TA Q500 thermogravimetric analyzer. The temperature degradation and change in weight of the samples with increasing temperature were observed by using TGA in a nitrogen atmosphere. The DSC TA-Q series 2000 instrument was used to study the thermal properties of the PLA/HC composite films. The DSC thermograms for the PLA/HC films were obtained for heating and cooling cycles at a heating rate of 10 °C/min from −20 to +200 °C under a nitrogen atmosphere.

2.6. Mechanical Property Testing. The mechanical properties of the PLA/HC composite films were performed using a uniaxial tensile test following the ASTM D882-10 standard for polymer films

https://doi.org/10.1021/acssusresmgt.4c00282
ACS Sustainable Resour. Manage. XXXX, XXX, XXX−XXX

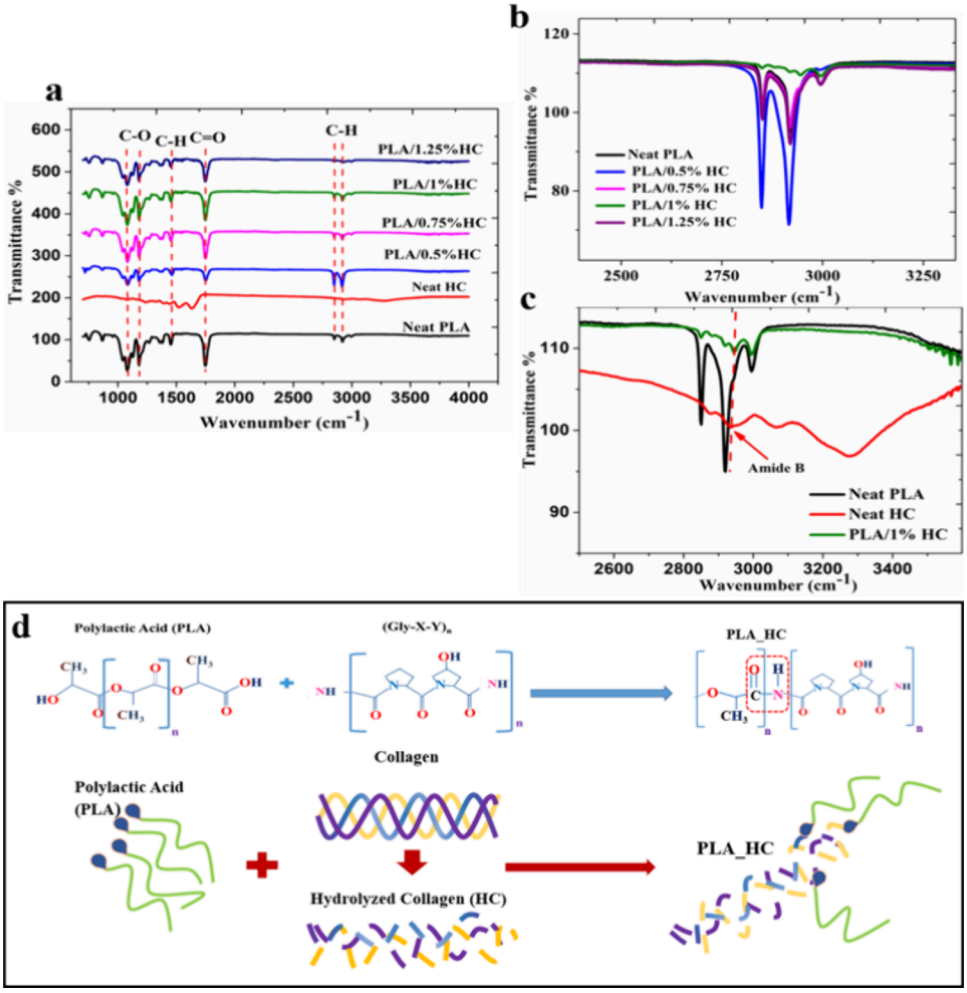

Figure 3. (a) FTIR spectrum of PLA/HC composite blown films (0.5, 0.75, 1, and 1.25 wt %) compared with neat PLA film and HC powder. (b and c) Magnified region of the FTIR spectrum from 2500−3400 cm^{-1}. (d) Schematic of possible chemical bonding between PLA and HC.

of less than 1 mm thickness. The average thickness of the films was measured at different points by using a digital vernier caliper with 0.001 mm resolution for reliable results. The 0.04−0.05 mm thickness × 150 mm length polymer film samples were placed between the upper and lower wedge grips of the Zwick/Roell Z2.5 universal testing machine. A load cell of 2.5 kN and a constant crosshead speed of 50 mm/min were set for the tensile testing of different composite polymer samples in the universal testing machine.

3. RESULTS AND DISCUSSION

3.1. Characterization of Hydrolyzed Collagen Powder. *3.1.1. XRD.* The material analysis of hydrolyzed collagen powder was performed using various characterization techniques, as shown in Figure 2. The XRD pattern of HC shows (Figure 2a) a prominent intensity peak at 2θ = 5° and a prominent broad peak at 2θ = 20° that characterize an amorphous material. It has been reported that, in neat collagen, the peak at 5° represents the distance between the molecular chains and the peak at 20° indicates the diffuse scattering.[31,32]

3.1.2. Raman Spectroscopy. Figure 2b gives the Raman analysis obtained for the HC that showed collagen and no collagenous moieties at 1250−1350 cm^{-1} (amide III) and 1590−1700 cm^{-1} (amide I) in the spectrum. The peak at 2945 cm^{-1} corresponds to a strong vibrational mode corresponding to the bending and stretching of the C−H groups. The hydrolysis process of collagen can result in a continuous change in the hydrogen-bonding structure as a function of separation between the collagen triple helices that cause a change in the O−H and N−H vibrational modes measured at the 3100−3500 cm^{-1} range.[33,34]

3.1.3. FTIR Spectroscopy. The types of functional groups and bonding in the HC were analyzed using FTIR spectroscopy, as shown in Figure 2c. The absorption peaks in the spectrum are associated with the bending and stretching of specific functional groups. The characteristic FTIR peaks obtained at 3275, 2924, 1635, 1522, and 1232 cm^{-1} correspond to amide A (N−H stretching), amide B (C−H stretching), amide I (N−H group bending vibration), amide II (C−N group stretching), and amide III (C−N stretching and N−H deformation), respectively. The absorption intensities of amide III (1232 cm^{-1}) and amide II (1450−1522 cm^{-1}) infer that the triple-helical structure arrangement of the collagen showed good agreement with the Raman spectrum obtained for HC.[35,36]

3.1.4. TGA. Figure 2d shows the thermal degradation study of the HC carried out until 900 °C with an initial degradation temperature of 282.32 °C, the first derivative peak temperature at 327.68 °C, and the complete material loss achieved at 900 °C. The surface morphology of the HC is included in Supporting Information S1 (see Figure S1).

https://doi.org/10.1021/acssusresmgt.4c00282
ACS Sustainable Resour. Manage. XXXX, XXX, XXX−XXX

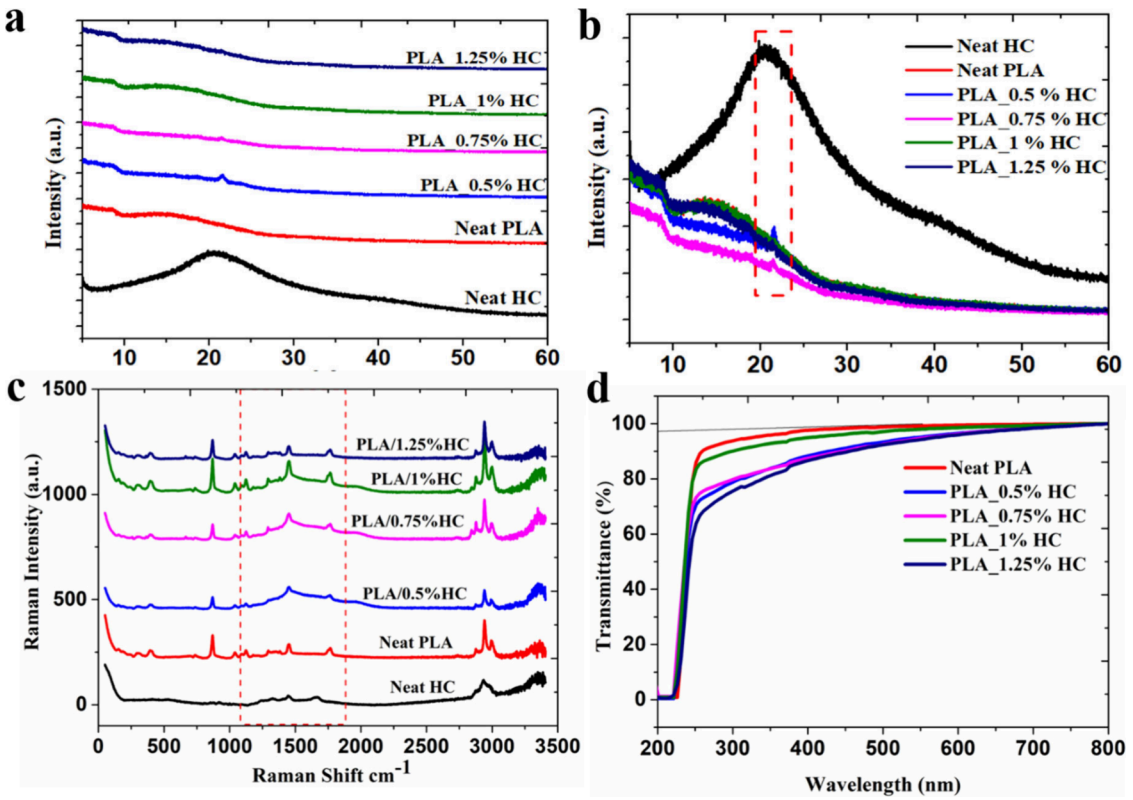

Figure 4. (a and b) XRD analysis, (c) Raman spectroscopy, and (d) UV−visible spectroscopy of PLA/HC composite blown films (0.5, 0.75, 1, and 1.25 wt %) compared with neat PLA and HC powder.

3.2. Characterization of PLA/HC Blown Films.

3.2.1. FTIR Spectroscopy. The interaction of the HC with the PLA polymer in the composite was further investigated by using FTIR analysis. Figure 3a compares the FTIR spectra obtained for neat PLA, hydrolyzed collagen, and composite blown films of PLA/HC 0.5 wt %, PLA/HC 0.75 wt %, PLA/HC 1.0 wt %, and PLA/HC 1.25 wt %. All of the HC/PLA composite films exhibited the characteristic peaks of the PLA polymer. It can be observed that neat PLA has weak peaks of −CH stretching vibrations at 2917 and 2845 cm^{-1}. The peaks at 1748 and 1452 cm^{-1} are attributed to the presence of −C═O of the ester bond and −CH bending vibrations. The other peaks at 1372, 1077, and 873 cm^{-1} correspond to −CH bending, $-CH_3$ stretching, and C−COO, respectively.[37,38] From Figure 3a, the FTIR spectra obtained for neat PLA and PLA/HC composite films were identical but with a significant decrease in the intensities of the peaks. Parts b and c of Figure 3 shows the CH stretching vibration region of the spectrum around 2500−3200 cm^{-1}. It was observed that PLA/HC 1% exhibited significant changes in this region compared with other weight percentages of HC blown films. A significant reduction of the C−H intensity peaks and an additional peak corresponding to amide B of the HC was observed for the 1% HC film (Figure 3c), showing strong chemical bonds with the PLA backbone. Zhang et al.[39] reported that PLA can form strong hydrogen bonds during polymer blending. Collagen, a natural polymer and a hydrogen donor, can form hydrogen bonds with PLA, which are weak secondary molecules but can hold the polymer molecules together.[40] Because the C−H groups can also act as donors for hydrogen bonds,[41] it was understood that the C−H groups in PLA have contributed to the hydrogen bonding between the collagen and PLA backbone, which resulted in a significant reduction of the intensities of the C−H peaks. Qin et al.[42] reported a similar intensity reduction in the FTIR spectrum of PLA-incorporated oil films due to the interaction of essential oils with the PLA functional groups. It has also been reported that the reduced peak intensities of the PLA/HC polymer films compared with neat PLA films can be attributed to the grafting of the filler to the polymer backbone.[43] Figure 3d gives the possible chemical interaction between PLA and HC during the composite formation. Ma et al.[44] reported the possible grafting reaction between the collagen and PLA from NMR spectral analysis. It was understood that chemical grafting occurs through a condensation reaction of the −NH and −COOH end groups in the collagen and PLA molecules. Because the weight percentage of HC in the polymer composite is very low to PLA, fewer grafting reactions occur in the composite. This finding can be correlated to the FTIR results obtained for the PLA_1% HC composite films. Endo et al.[45] also reported that the intermolecular interaction of PLA and collagen is due to the inter-hydrogen bonding of −OH−O═, −NH−O═, and −CH−O═ functional groups from frontier molecular orbital theory calculations. It can be inferred that, as a natural polymer, the amides in the HC helped to be covalently grafted to the backbone of PLA, forming the PLA/HC composites.

3.2.2. Raman Spectroscopy. The Raman spectra (Figure 4c) of the neat PLA and composite films were compared to confirm the interaction with HC and PLA during composite formation. Neat PLA has peaks at 867, 1024, 1190, 1297, 1385, 1762, and 2846−3000 cm^{-1}, which correspond to −C−COO, $-C-CH_3$, CH_3, CH, CH_3, −C═O, and −CH vibrational groups, respectively.[46] In the HC Raman spectrum around 1000−2000 cm^{-1} (Figure 2b), the broad peak corresponds to

https://doi.org/10.1021/acssusresmgt.4c00282
ACS Sustainable Resour. Manage. XXXX, XXX, XXX−XXX

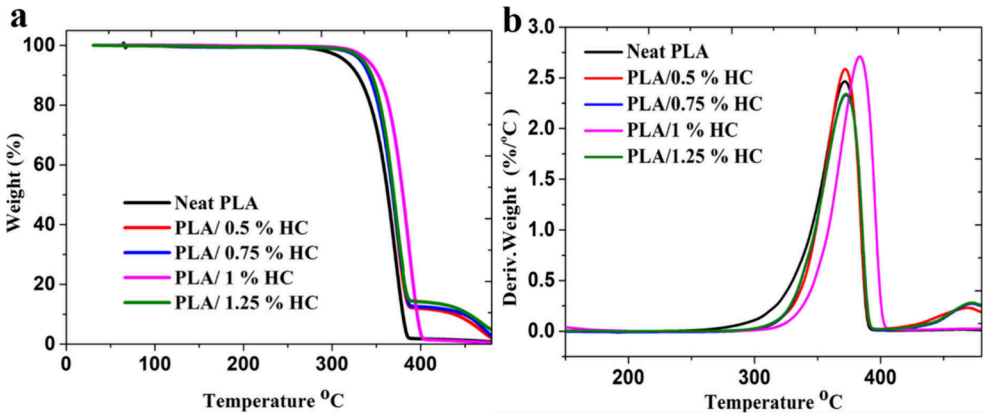

Figure 5. (a) TGA and (b) DTG curves obtained for different PLA/HC composite blown films.

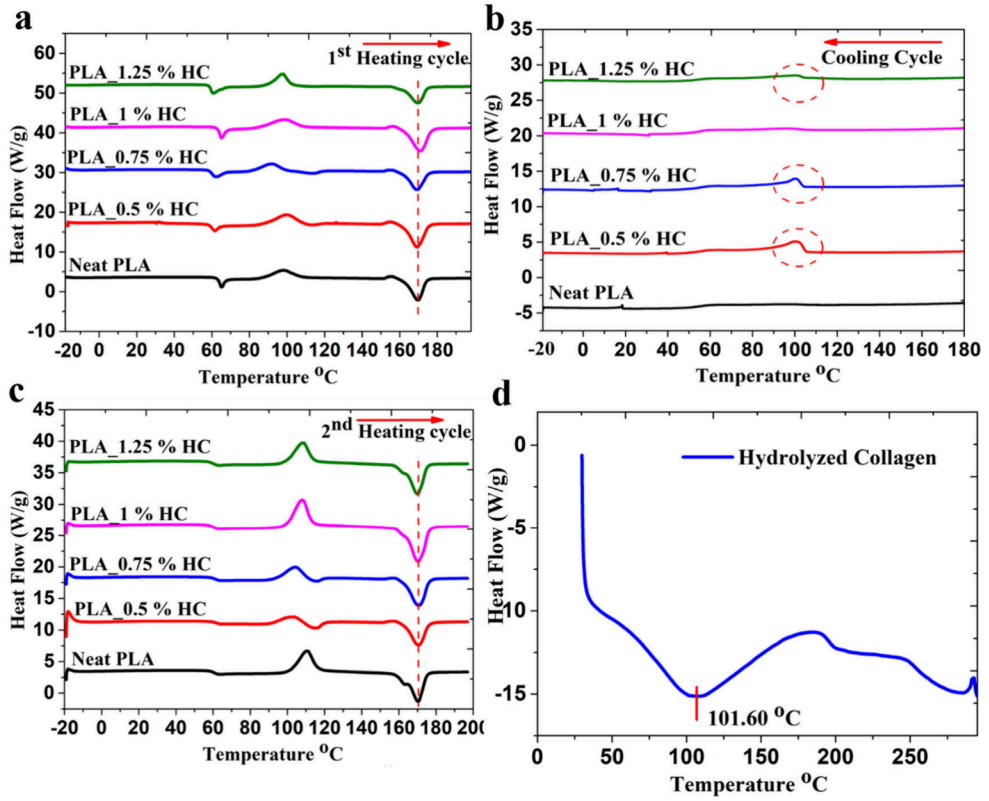

Figure 6. DSC analysis of different concentrations of PLA/HC blown films compared with the neat PLA film: (a) during the first heating cycle; (b) during the cooling cycle; (c) during the second heating cycle. (d) DSC curve for hydrolyzed collagen powder.

amide III and amide I, whereas PLA corresponds to the C−H groups. Figure 4c shows that, compared with the neat PLA film, there was a broad bend in the spectrum in the C−H region of the PLA composite films exhibiting an interaction with amides in HC. The Raman spectra exhibited high intensity for PLA/1% HC peaks compared to neat PLA and other composite films in the CH regions around 1000−2000 and 2846−3000 cm^{-1}. The increased intensity can be correlated with the hydrogen bonding between PLA and HC. The amino acids and peptides in HC react with the PLA polymer chains and increase the peak intensities due to overlapping functional groups. The Raman spectrum infers that 1 wt % of HC in PLA was the optimized concentration that gives better grafting with the PLA polymer backbone. The broken-down amino acids and peptides in the HC act as nucleating agents in PLA, further improving the crystallinity of the PLA/HC composite films.[47]

3.2.3. XRD. To analyze the interaction of HC in the PLA matrix, XRD of the PLA/HC films was taken. Parts a and b of Figure 4 show the XRD patterns obtained for the blown films with different weight percentages of HC in PLA. Neat PLA possesses a broad peak maximum of approximately $2\theta = 16°$, and all of the composite films exhibited the characteristic peak of PLA in the spectrum. PLA/HC films with 05, 0.75, and 1.25 wt % clearly show the distinctive peak of HC, with a slight shift toward the right at $2\theta = 21°$ shown in Figure 4b. The HC peak's right shift can probably be due to thermal expansion during the filament and film extrusion processes. Interestingly, the HC peak was not observed in the PLA/1% HC, confirming

https://doi.org/10.1021/acssusresmgt.4c00282
ACS Sustainable Resour. Manage. XXXX, XXX, XXX−XXX

that the HC was miscible in the PLA matrix forming the PLA/HC blend.

3.2.4. UV–Visible Spectroscopy. In the field of food-packaging applications, it is indispensable to analyze the UV-blocking performance and transparency of polymer composite films. It has been reported that the addition of fillers in a polymer matrix can alter the transparency and reduce the passage of UV radiation through the polymer composite films.[48,49] Figure 4d shows PLA composite films analyzed using UV–visible spectroscopy. The neat PLA films exhibited maximum transparency with a transmittance of 92% in the UV–visible region. The spectrum reveals the reduction of transparency by adding HC in neat PLA. The composite films with 1, 0.75, 0.5, and 1.25 wt % of HC in PLA indicate transparency of 87%, 76%, 73%, and 68%, respectively. It was noticeable that, compared to other HC weight percentages in PLA, 1 wt % indicated maximum transparency, confirming the complete miscibility of HC in the PLA matrix. Therefore, UV–visible spectroscopy analysis confirms that the PLA/HC composite films are UV-protective and can be potentially used for food-packaging applications.[50] The surface morphology analysis of the neat PLA and PLA/HC composite blown film samples using SEM is given in Supporting Information S2 (see Figure S2).

3.3. Thermal Property Analysis of PLA/HC Blown Films. *3.3.1. TGA.* Parts a and b of Figure 5 give the percentage of weight degradation curves (TGA) and derivative weight percentage curves (differential thermogravimetry, DTG) of different PLA/HC films for an increase in temperature from 30 to 500 °C.

The initial, final, and significant decomposition temperatures obtained from the TGA characteristic curves for neat PLA and different PLA/HC composite films are summarized in Table S1. All of the PLA/HC composite films showed an enhancement in the initial decomposition temperature compared to neat PLA, which infers improvement in the thermal stability of the films. It has been reported that adding natural sources to polymer composites can enhance their thermal stability.[51,52] The thermograms showed a single-step degradation for neat PLA film and PLA/1% HC at 385 and 400 °C, respectively, whereas PLA/0.5% HC, PLA/0.75% HC, and PLA/1.25% HC films decomposed through a two-stage process, where the first step is attributed to the PLA matrix and the second step is exhibited by the presence of HC, which completely decomposes at 500 °C.[53]

The TGA curve of HC in Figure 2d confirms good thermal stability at high temperatures, further improving the thermal stability of the PLA/HC composite. A significant increase in the initial, final, and major degradation temperatures was observed in the PLA/1 wt % HC composite film, attributed to better HC compatibility in PLA compared to 0.5, 0.75, and 1.25 wt % of HC in composite films. The TGA curve validates the uniform dispersion and grafting of 1 wt % of HC in PLA under solution blending with an enhanced temperature profile compared to the neat PLA film.

3.3.2. DSC. The crystallinity behavior of the PLA/HC composite films was investigated by using DSC analysis. Parts a–c of Figure 6 give the DSC thermograms obtained for the first, cooling, and second heating cycles. Based on the first heating cycle, the crystallinity (χ_c) of the composite film samples was calculated using the equation[54]

$$\chi_c = \frac{\Delta H_m - \Delta H_c}{W \Delta H^\circ_m} \quad (1)$$

where ΔH_m is the crystallization enthalpy of the samples (J/g), ΔH_c is the cold crystallization enthalpy, ΔH°_m represents the melting enthalpy of 100% crystalline PLA, that is, 93.7 J/g, and w is the weight fraction of PLA. Figure 6d gives the DSC thermogram of neat HC showing thermal stability with an endothermic peak at 101.6 °C.

The values obtained for glass transition temperatures (T_g), cold crystallization temperatures (T_c), melting temperatures (T_m), and melting enthalpy (ΔH_m) of the polymer samples are summarized in Table S2. In the first heating cycle, it was observed that 0.5%, 0.75%, and 1.25% HC in PLA composite films exhibited a noticeable shift in T_g values to lower temperatures compared to neat PLA, whereas 1% HC exhibited a value near that of neat PLA. The increase in the glass transition temperature by 1% HC compared to other weight percentages can be attributed to the intermolecular interaction of the hydrogen bonds in the blend.[53] However, in 0.5%, 0.75%, and 1.25% HC composite films, the low molecular weight of the HC caused a reduction in the intermolecular interaction with the PLA chains, which was attributed to a decrease in T_g. It was also observed that the T_g peaks showed a sharp overshoot in the thermograms, indicating a physical aging phenomenon, particularly in the polymer composite films.[55] The cold crystallization peak obtained for 0.5%, 0.75%, 1%, and 1.25% HC in the PLA composite films in the first and second heating cycles shifted to higher temperatures than the neat PLA films. It has been reported that this phenomenon is due to the faster crystallization by the influence of fillers, which act as nucleating agents of the PLA polymer.[56,57]

From the first to second heating cycle, T_m for all of the polymer film samples showed a shift of 1 °C. In the second heating cycle, the T_g peak was almost absent because of the irreversible crystallization during the first heating cycle.[58] After the first heating cycle, followed by a cooling cycle, the amorphous phases were reduced and more crystalline phases were formed. It was reported that PLA does not exhibit a crystallization peak at a faster cooling rate (10 °C/min) in the first cooling cycle because of the slow crystallization rate.[59,60] An exothermic peak was observed during the first cooling cycle (Figure 6b) in 0.5, 0.75, and 1.25 wt % HC polymer composite and was almost absent in 1 wt % HC and neat PLA films. The exothermic peak observed during the cooling cycle was attributed to the crystallization behavior of PLA due to nucleation and cross-linking.[61] The DSC thermogram was obtained for 0.5, 0.75, and 1.25 wt % HC, and 1 wt % HC exhibits a significant difference in the results. It was understood that, at 0.5, 0.75, and 1.25 wt %, HC has a strong nucleation effect that promotes a crystallization peak, whereas the optimized 1 wt % exhibits strong cross-linking with the PLA matrix that blocks the movement of PLA chains to reduce crystallization during the cooling cycle. The increase in the melting temperature also confirms the cross-linking of PLA and HC of 1%.

During the second heating cycle, the crystalline phases melt at a lower temperature, resulting in a lower melting temperature shift in the composite samples. Adding HC as a filler reduced the crystallinity of the composites, confirming that the filler acted as a nucleating agent in the PLA matrix.[62,63] It was interesting to observe that the crystallinity of the PLA/

https://doi.org/10.1021/acssusresmgt.4c00282
ACS Sustainable Resour. Manage. XXXX, XXX, XXX–XXX

HC composite with 1% filler showed high crystallinity, due to the optimized percentage in the PLA matrix with cross-linking. It was understood that the increase in crystallinity was due to the proper reinforcement of the low-molecular-weight HC particle in the PLA matrix.[64]

3.4. Mechanical Property Analysis of PLA/HC Blown Films.

Figure 7 shows the tensile characteristics obtained for PLA/HC composite blown films at 0.5, 0.75, 1.0, and 1.25 wt % HC in the PLA matrix. PLA has an inherent fracture brittle characteristic, and adding HC in PLA has significantly improved the elongation strength of the PLA composite. The PLA/0.5% HC, PLA/0.75% HC, and PLA/1.25% HC composite films exhibited elastomer characteristics with low tensile strength and very high elongation strength in tensile curves b, c, and e, respectively. The tensile strength and elongation at break values obtained for the PLA composite samples are summarized in Table S3. The PLA/1% HC sample showed a remarkable increase in tensile strength and elongation strength compared to the other composite films. Generally, the filler materials in the PLA matrix decrease the tensile modulus and tensile strength and increase the elongation strength of the composite.[65,66] The mechanical property analysis indicates that the HC filler significantly increased the toughness of PLA and 1 wt % HC in PLA contributed to the excellent elongation and tensile strength.

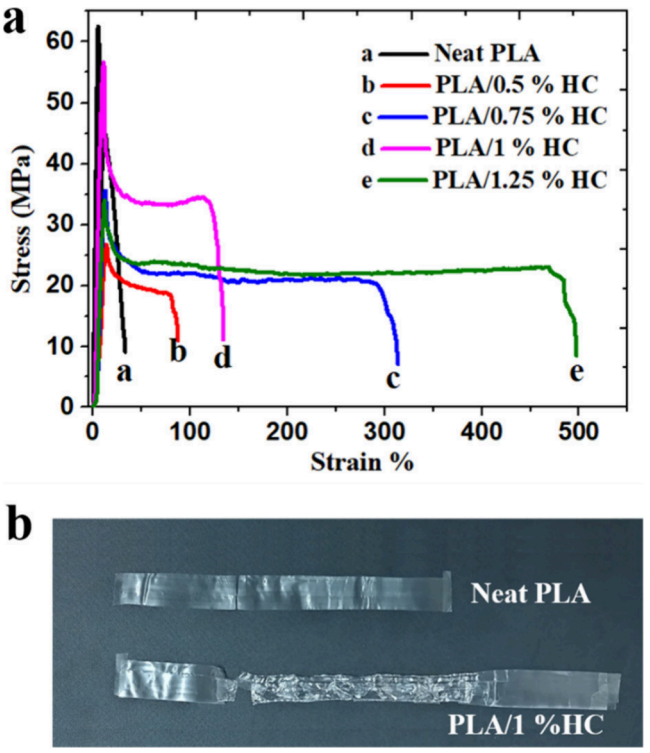

Figure 7. (a) Stress versus strain curves obtained for neat PLA and PLA/HC composite blown films. (b) Neat PLA and PLA/1% HC blown films after tensile testing.

Galuska et al.[67] reported that incorporating hydrogen bonds in the backbone of polymer chains is an effective strategy to enhance the mechanical performance of the polymer. The study agrees with the improved mechanical performance of PLA/HC composite films. They reported that increased hydrogen bonds in the polymer matrix may result in plasticization of the films. The elongation at break for the PLA/HC composite films increased with the HC concentration, and 1.25% HC exhibited the maximum elongation at break. HC as an amorphous material incorporated in semiamorphous PLA reduced the crystallinity, causing excellent flexibility for the PLA/HC composite films. The formation of hydrogen bonds and the amide bonding in PLA/1% HC further increased the crystallinity and exhibited excellent tensile strength and elongation at break. Figure 7b shows neat PLA and PLA/1% HC blown-film samples after the tensile test performed under ASTM -D882. Fracture analysis of neat PLA and PLA/HC composite films using SEM is explained in Supporting Information S3 (see Figure S3).

4. CONCLUSIONS

PLA/HC biocomposites with different weight percentages (0.5, 0.75, 1, and 1.25 wt %) of HC in PLA were prepared using solution blending, and the PLA/HC biocomposite films were prepared using a blown-film extrusion technique. The Raman and FTIR analyses of the composite films reveal the chemical interaction of the amide group and the formation of hydrogen bonds between the HC and PLA matrix. The investigation on the PLA/HC composite infers that the HC with a low molecular weight of 3−6 kDa can reinforce the PLA backbone, thereby improving the flexibility of the PLA/HC biocomposite. PLA/1% HC was the optimized concentration, forming a PLA/HC blend with excellent thermal and mechanical properties. TGA shows that the initial and final degradation temperatures were enhanced at 1 wt % HC in PLA. The different concentrations of HC in PLA 1 wt % exhibit an excellent tensile strength of 52 MPa and 1.25 wt % with an excellent elongation strength of 476.2% compared to neat PLA films. It can be concluded that the HC-reinforced PLA film from renewable resources with better thermal stability, excellent mechanical properties, and inherent biodegradable properties can be employed for packaging applications with further studies.

■ ASSOCIATED CONTENT

Supporting Information

The Supporting Information is available free of charge at https://pubs.acs.org/doi/10.1021/acssusresmgt.4c00282.

Morphology and surface analysis of the HC imaged using FE-SEM (Figure S1), surface morphology of the neat PLA and PLA/HC composite blown-film samples using FE-SEM (Figure S2), fracture surface analysis of the tensile-tested neat PLA and PLA/1% HC blown-film samples using FE-SEM (Figure S3), summary of the TGA results obtained for PLA/HC films (Table S1), summary of the DSC results obtained for PLA/HC films (Table S2), and summary of the data obtained from tensile studies of the PLA/HC films (Table S3) (PDF)

■ AUTHOR INFORMATION

Corresponding Author

Vijay K. Rangari − *Department of Material Science and Engineering, Tuskegee University, Tuskegee, Alabama 36088, United States;* orcid.org/0000-0002-3962-1686; Email: vrangari@tuskegee.edu

https://doi.org/10.1021/acssusresmgt.4c00282
ACS Sustainable Resour. Manage. XXXX, XXX, XXX−XXX

Author

Radhika Panickar − *Department of Material Science and Engineering, Tuskegee University, Tuskegee, Alabama 36088, United States*

Complete contact information is available at: https://pubs.acs.org/10.1021/acssusresmgt.4c00282

Notes

The authors declare no competing financial interest.

■ ACKNOWLEDGMENTS

The authors acknowledge financial support from AL-EPSCoR (1655280), NSF CREST (1735971), and DMR (2117242). We thank Dr. Lakshmi V. Nair for helping with the UV−visible spectroscopy of the film samples.

■ REFERENCES

(1) Kibria, M. G.; Masuk, N. I.; Safayet, R.; Nguyen, H. Q.; Mourshed, M. Plastic Waste: Challenges and Opportunities to Mitigate Pollution and Effective Management. *Int. J. Environ. Res.* **2023**, *17* (1), 20.

(2) Evode, N.; Qamar, S. A.; Bilal, M.; Barceló, D.; Iqbal, H. M. N. Plastic Waste and Its Management Strategies for Environmental Sustainability. *Case Stud. Chem. Environ. Eng.* **2021**, *4*, 100142.

(3) Lebreton, L.; Andrady, A. Future Scenarios of Global Plastic Waste Generation and Disposal. *Palgrave Commun.* **2019**, *5* (1), 6.

(4) Long, H.; Wang, S.; Wu, W.; Zhang, G. The Economic Influence of Oil Shortage and the Optimal Strategic Petroleum Reserve in China. *Energy Reports* **2022**, *8*, 9858−9870.

(5) Miller, R. G.; Sorrell, S. R. The Future of Oil Supply. *Philos. Trans. Ser. A, Math. Phys. Eng. Sci.* **2014**, *372* (2006), 20130179.

(6) Moshood, T. D.; Nawanir, G.; Mahmud, F.; Mohamad, F.; Ahmad, M. H.; AbdulGhani, A. Biodegradable Plastic Applications towards Sustainability: A Recent Innovations in the Green Product. *Clean. Eng. Technol.* **2022**, *6*, 100404.

(7) Rosenboom, J.-G.; Langer, R.; Traverso, G. Bioplastics for a Circular Economy. *Nat. Rev. Mater.* **2022**, *7* (2), 117−137.

(8) Moshood, T. D.; Nawanir, G.; Mahmud, F.; Mohamad, F.; Ahmad, M. H.; AbdulGhani, A. Sustainability of Biodegradable Plastics: New Problem or Solution to Solve the Global Plastic Pollution? *Curr. Res. Green Sustain. Chem.* **2022**, *5*, 100273.

(9) DeStefano, V.; Khan, S.; Tabada, A. Applications of PLA in Modern Medicine. *Eng. Regen.* **2020**, *1*, 76−87.

(10) Balla, E.; Daniilidis, V.; Karlioti, G.; Kalamas, T.; Stefanidou, M.; Bikiaris, N. D.; Vlachopoulos, A.; Koumentakou, I.; Bikiaris, D. N. Poly(Lactic Acid): A Versatile Biobased Polymer for the Future with Multifunctional Properties—From Monomer Synthesis, Polymerization Techniques and Molecular Weight Increase to PLA Applications. *Polymers (Basel).* **2021**, *13* (11), 1822.

(11) Lim, L.-T.; Auras, R.; Rubino, M. Processing Technologies for Poly(Lactic Acid). *Prog. Polym. Sci.* **2008**, *33* (8), 820−852.

(12) Lansing, E.; Sains, U. Poly (Lactic Acid)—Mass Production, Processing, Industrial Applications, and End of Life. *Adv. Drug Delivery Rev.* **2016**, 1−161.

(13) Madhavan Nampoothiri, K.; Nair, N. R.; John, R. P. An Overview of the Recent Developments in Polylactide (PLA) Research. *Bioresour. Technol.* **2010**, *101* (22), 8493−8501.

(14) Jem, K. J.; Tan, B. The Development and Challenges of Poly (Lactic Acid) and Poly (Glycolic Acid). *Adv. Ind. Eng. Polym. Res.* **2020**, 3 (2), 60−70.

(15) Tan, B. H.; Muiruri, J. K.; Li, Z.; He, C. Recent Progress in Using Stereocomplexation for Enhancement of Thermal and Mechanical Property of Polylactide. *ACS Sustain. Chem. Eng.* **2016**, *4* (10), 5370−5391.

(16) Luo, F.; Fortenberry, A.; Ren, J.; Qiang, Z. Recent Progress in Enhancing Poly(Lactic Acid) Stereocomplex Formation for Material Property Improvement. *Front. Chem.* **2020**, *8* (688). DOI: 10.3389/fchem.2020.00688.

(17) Bhardwaj, R; Mohanty, A. K. Advances in the Properties of Polylactides Based Materials: A Review. *J. Biobased Mater. Bioenergy* **2007**, *1*, 191−209.

(18) Deeraj, B. D. S.; Jayan, J. S.; Saritha, A.; Joseph, K. 8-PLA-Based Blends and Composites. In *Biodegradable Polymers, Blends, and Composites*; Woodhead Publishing Series in Composites Science and Engineering; Woodhead Publishing, 2022; pp 237−281. DOI: 10.1016/B978-0-12-823791-5.00014-4.

(19) Zhao, X.; Yu, J.; Liang, X.; Huang, Z.; Li, J.; Peng, S. Crystallization Behaviors Regulations and Mechanical Performances Enhancement Approaches of Polylactic Acid (PLA) Biodegradable Materials Modified by Organic Nucleating Agents. *Int. J. Biol. Macromol.* **2023**, *233*, 123581.

(20) Shi, K.; Liu, G.; Sun, H.; Yang, B.; Weng, Y. Effect of Biomass as Nucleating Agents on Crystallization Behavior of Polylactic Acid. *Polymers (Basel)* **2022**, *14* (20), 4305.

(21) Samir, A.; Ashour, F. H.; Hakim, A. A. A.; Bassyouni, M. Recent Advances in Biodegradable Polymers for Sustainable Applications. *npj Mater. Degrad.* **2022**, *6* (1), 68.

(22) Hamdani, S.; Longuet, C.; Lopez-Cuesta, J.-M.; Ganachaud, F. Calcium and Aluminium-Based Fillers as Flame-Retardant Additives in Silicone Matrices. I. Blend Preparation and Thermal Properties. *Polym. Degrad. Stab.* **2010**, *95* (9), 1911−1919.

(23) Anita Lett, J.; Sagadevan, S.; Fatimah, I.; Hoque, M. E.; Lokanathan, Y.; Léonard, E.; Alshahateet, S. F.; Schirhagl, R.; Oh, W. C. Recent Advances in Natural Polymer-Based Hydroxyapatite Scaffolds: Properties and Applications. *Eur. Polym. J.* **2021**, *148*, 110360.

(24) Gorna, K.; Hund, M.; Vučak, M.; Gröhn, F.; Wegner, G. Amorphous Calcium Carbonate in Form of Spherical Nanosized Particles and Its Application as Fillers for Polymers. *Mater. Sci. Eng. A* **2008**, *477* (1), 217−225.

(25) Baldanov, A.B.; Bokhoeva, L.A.; Shalbuev, D.V.; Tumurova, T.B. Collagen Based Bio-Additives in Polymer Composites. *Nanotekhnologii v Stroit.* **2022**, *14*, 137.

(26) Sionkowska, A. Collagen Blended with Natural Polymers: Recent Advances and Trends. *Prog. Polym. Sci.* **2021**, *122*, 101452.

(27) León-López, A.; Morales-Peñaloza, A.; Martínez-Juárez, V. M.; Vargas-Torres, A.; Zeugolis, D. I.; Aguirre-Álvarez, G. Hydrolyzed Collagen-Sources and Applications. *Molecules* **2019**, *24* (22), 4031.

(28) Dewey, M. J.; Johnson, E. M.; Weisgerber, D. W.; Wheeler, M. B.; Harley, B. A. C. Shape-Fitting Collagen-PLA Composite Promotes Osteogenic Differentiation of Porcine Adipose Stem Cells. *J. Mech. Behav. Biomed. Mater.* **2019**, *95*, 21−33.

(29) Martin, V.; Ribeiro, I. A.; Alves, M. M.; Gonçalves, L.; Claudio, R. A.; Grenho, L.; Fernandes, M. H.; Gomes, P.; Santos, C. F.; Bettencourt, A. F. Engineering a Multifunctional 3D-Printed PLA-Collagen-Minocycline-NanoHydroxyapatite Scaffold with Combined Antimicrobial and Osteogenic Effects for Bone Regeneration. *Mater. Sci. Eng. C* **2019**, *101*, 15−26.

(30) Xie, Y.; Zhang, F.; Akkus, O.; King, M. W. A Collagen/PLA Hybrid Scaffold Supports Tendon-Derived Cell Growth for Tendon Repair and Regeneration. *J. Biomed. Mater. Res. B. Appl. Biomater.* **2022**, *110* (12), 2624−2635.

(31) Silva, C.C; Thomazini, D; Pinheiro, A.G; Aranha, N; Figueiro, S.D; Góes, J.C; Sombra, A.S.B Collagen-Hydroxyapatite Films: Piezoelectric Properties. *Mater. Sci. Eng. B* **2001**, *86* (3), 210−218.

(32) Sun, T. W.; Zhu, Y. J.; Chen, F. Hydroxyapatite Nanowire/Collagen Elastic Porous Nanocomposite and Its Enhanced Performance in Bone Defect Repair. *RSC Adv.* **2018**, *8* (46), 26218−26229.

(33) Leikin, S.; Parsegian, V. A.; Yang, W. H.; Walrafen, G. E. Raman Spectral Evidence for Hydration Forces between Collagen Triple Helices. *Proc. Natl. Acad. Sci. U. S. A.* **1997**, *94* (21), 11312−11317.

(34) Buchwald, T.; Kozielski, M.; Szybowicz, M. Determination of Collagen Fibers Arrangement in Bone Tissue by Using Trans-

formations of Raman Spectra Maps. *Spectrosc. (New York)* **2012**, *27* (2), 107−117.
(35) Riaz, T.; Zeeshan, R.; Zarif, F.; Ilyas, K.; Muhammad, N.; Safi, S. Z.; Rahim, A.; Rizvi, S. A. A.; Rehman, I. U. FTIR Analysis of Natural and Synthetic Collagen. *Appl. Spectrosc. Rev.* **2018**, *53* (9), 703−746.
(36) Sripriya, R.; Kumar, R. A Novel Enzymatic Method for Preparation and Characterization of Collagen Film from Swim Bladder of Fish Rohu (*Labeo Rohita*). *Food Nutr. Sci.* **2015**, *06* (15), 1468−1478.
(37) Awale, R. J.; Ali, F. B.; Azmi, A. S.; Puad, N. I. M.; Anuar, H.; Hassan, A. Enhanced Flexibility of Biodegradable Polylactic Acid/Starch Blends Using Epoxidized Palm Oil as Plasticizer. *Polymers (Basel).* **2018**, *10* (9), 977.
(38) Ficai, A.; Albu, M. G.; Birsan, M.; Sonmez, M.; Ficai, D.; Trandafir, V.; Andronescu, E. Collagen Hydrolysate Based Collagen/Hydroxyapatite Composite Materials. *J. Mol. Struct.* **2013**, *1037*, 154−159.
(39) Zhang, Y.; Chen, J.; Peng, Q.; Song, L.; Wang, Z.; Wang, Z. Hydrogen Bonding Assisted Toughness Enhancement of Poly-(Lactide) Blended with a Bio-Based Polyamide Elastomer of Extremely Low Amounts. *Appl. Surf. Sci.* **2020**, *506*, 144684.
(40) Sionkowska, A.; Skopinska-Wisniewska, J.; Wisniewski, M. Collagen-Synthetic Polymer Interactions in Solution and in Thin Films. *J. Mol. Liq.* **2009**, *145* (3), 135−138.
(41) Derewenda, Z. S. C-H Groups as Donors in Hydrogen Bonds: A Historical Overview and Occurrence in Proteins and Nucleic Acids. *Int. J. Mol. Sci.* **2023**, *24* (17), 13165.
(42) Qin, Y.; Li, W.; Liu, D.; Yuan, M.; Li, L. Development of Active Packaging Film Made from Poly (Lactic Acid) Incorporated Essential Oil. *Prog. Org. Coatings* **2017**, *103*, 76−82.
(43) Shazleen, S. S.; Foong Ng, L. Y.; Ibrahim, N. A.; Hassan, M. A.; Ariffin, H. Combined Effects of Cellulose Nanofiber Nucleation and Maleated Polylactic Acid Compatibilization on the Crystallization Kinetic and Mechanical Properties of Polylactic Acid Nanocomposite. *Polymers (Basel).* **2021**, *13* (19), 3226.
(44) Ma, H.; Shen, J.; Yang, Q.; Zhou, J.; Xia, S.; Cao, J. Effect of the Introduction of Fish Collagen on the Thermal and Mechanical Properties of Poly(Lactic Acid). *Ind. Eng. Chem. Res.* **2015**, *54* (43), 10945−10951.
(45) Endo, K.; Fuse, M.; Kato, N. Interactions b/w Collagen and Polylactic-Acid Molecular Models Due to DFT Calculations. *J. Biomed. Res. Environ. Sci.* **2022**, *3* (5), 537−546.
(46) Gan, L.; Geng, A.; Jin, L.; Zhong, Q.; Wang, L.; Xu, L.; Mei, C. Antibacterial Nanocomposite Based on Carbon Nanotubes-Silver Nanoparticles-Co-Doped Polylactic Acid. *Polym. Bull.* **2020**, *77* (2), 793−804.
(47) Carbone, M. J.; Vanhalle, M.; Goderis, B.; Van Puyvelde, P. Amino Acids and Poly(Amino Acids) as Nucleating Agents for Poly(Lactic Acid). *J. Polym. Eng.* **2015**, *35* (2), 169−180.
(48) Kim, I.; Viswanathan, K.; Kasi, G.; Sadeghi, K.; Thanakkasaranee, S.; Seo, J. Poly (Lactic Acid)/ Zno Bionanocomposite Films with Positively Charged Zno as Potential Antimicrobial Food Packaging Materials. *Polymers (Basel)* **2019**, *11* (9), 1427.
(49) Roy, S.; Rhim, J. International Journal of Biological Macromolecules Preparation of Bioactive Functional Poly (Lactic Acid)/Curcumin Composite Fi Lm for Food Packaging Application. *Int. J. Biol. Macromol.* **2020**, *162*, 1780−1789.
(50) Mondal, K.; Soundararajan, N.; Goud, V. V.; Katiyar, V. Cellulose Nanocrystals Modulate Curcumin Migration in PLA-Based Active Films and Its Application as Secondary Packaging. *ACS Sustain. Chem. Eng.* **2024**, *12* (26), 9642−9657.
(51) Gbadeyan, O. J.; Linganiso, L. Z.; Deenadayalu, N. Thermomechanical Characterization of Bioplastic Films Produced Using a Combination of Polylactic Acid and Bionano Calcium Carbonate. *Sci. Rep.* **2022**, *12* (1), 1−9.
(52) Mohamad Haafiz, M. K.; Hassan, A.; Arjmandi, R.; Zakaria, Z.; Marliana, M. M.; Syakir, M. I.; Nurul Fazita, M. R. Microcrystalline Cellulose from Oil Palm Empty Fruit Bunches as Filler in Polylactic Acid. *Polym. Polym. Compos.* **2016**, *24* (9), 675−680.
(53) Lu, H.; Madbouly, S. A.; Schrader, J. A.; Srinivasan, G.; Mccabe, K. G.; Grewell, D.; Kessler, M. R.; Graves, W. R. Biodegradation Behavior of Poly(Lactic Acid) (PLA)/Distiller's Dried Grains with Solubles (DDGS) Composites. *ACS Sustain. Chem. Eng.* **2014**, *2* (12), 2699−2706.
(54) Wu, H.; Hou, A.; Qu, J. P. Phase Morphology and Performance of Supertough PLA/EMA-GMA/ZrP Nanocomposites Prepared through Reactive Melt-Blending. *ACS Omega* **2019**, *4* (21), 19046−19053.
(55) Hernández Sánchez, F.; Molina Mateo, J.; Romero Colomer, F. J.; Salmerón Sánchez, M.; Gómez Ribelles, J. L.; Mano, J. F. Influence of Low-Temperature Nucleation on the Crystallization Process of Poly(L-Lactide). *Biomacromolecules* **2005**, *6* (6), 3283−3290.
(56) Frone, A. N.; Berlioz, S.; Chailan, J. F.; Panaitescu, D. M. Morphology and Thermal Properties of PLA-Cellulose Nanofibers Composites. *Carbohydr. Polym.* **2013**, *91* (1), 377−384.
(57) Suryanegara, L.; Nakagaito, A. N.; Yano, H. The Effect of Crystallization of PLA on the Thermal and Mechanical Properties of Microfibrillated Cellulose-Reinforced PLA Composites. *Compos. Sci. Technol.* **2009**, *69* (7-8), 1187−1192.
(58) Yang, Z.; Peng, H.; Wang, W.; Liu, T. Crystallization Behavior of Poly(ε-Caprolactone)/Layered Double Hydroxide Nanocomposites. *J. Appl. Polym. Sci.* **2010**, *116* (5), 2658−2667.
(59) Farid, T.; Herrera, V. N.; Kristiina, O. Investigation of Crystalline Structure of Plasticized Poly (Lactic Acid)/Banana Nanofibers Composites. *IOP Conf. Ser. Mater. Sci. Eng.* **2018**, *369* (1), 012031.
(60) Jongpanya-Ngam, P.; Khankrua, R.; Seadan, M.; Suttiruengwong, S. Effect of Synthesized Sulfonate Derivatives as Nucleating Agents on Crystallization Behavior of Poly(Lactic Acid). *Des. Monomers Polym.* **2022**, *25* (1), 115−127.
(61) Guo, Z.; Song, W.; Wei, X.; Feng, Y.; Song, Y.; Guo, Z.; Cheng, W.; Miao, W.; Cheng, B.; Song, S. Effect of Matrix Composition on the Performance of Calcium Carbonate Filled Poly(Lactic Acid)/Poly(Butylene Adipate-Co-Terephthalate) Composites. *E-Polymers* **2023**, *23* (1), 20230026.
(62) Espinach, F. X.; Boufi, S.; Delgado-Aguilar, M.; Julián, F.; Mutjé, P.; Méndez, J. A. Composites from Poly(Lactic Acid) and Bleached Chemical Fibres: Thermal Properties. *Compos. Part B Eng.* **2018**, *134*, 169−176.
(63) Kodali, D.; Hembrick-Holloman, V.; Gunturu, D. R.; Samuel, T.; Jeelani, S.; Rangari, V. K. Influence of Fish Scale-Based Hydroxyapatite on Forcespun Polycaprolactone Fiber Scaffolds. *ACS Omega* **2022**, *7* (10), 8323−8335.
(64) Mustapa, I. R.; Shanks, R. A.; Kong, I. Melting Behaviour and Dynamic Mechanical Properties of Poly(Lactic Acid)-Hemp-Nanosilica Composites. *Asian Trans. Basic Appl. Sci.* **2013**, *3* (2), 29−37.
(65) Yu, M.; Zheng, Y.; Tian, J. Study on the Biodegradability of Modified Starch/Polylactic Acid (PLA) Composite Materials. *RSC Adv.* **2020**, *10* (44), 26298−26307.
(66) Pawlak, F.; Aldas, M.; López-Martínez, J.; Samper, M. D. Effect of Different Compatibilizers on Injection-Molded Green Fiber-Reinforced Polymers Based on Poly(Lactic Acid)-Maleinized Linseed Oil System and Sheep Wool. *Polymers (Basel).* **2019**, *11* (9), 1514.
(67) Galuska, L. A.; Ocheje, M. U.; Ahmad, Z. C.; Rondeau-Gagné, S.; Gu, X. Elucidating the Role of Hydrogen Bonds for Improved Mechanical Properties in a High-Performance Semiconducting Polymer. *Chem. Mater.* **2022**, *34* (5), 2259−2267.

https://doi.org/10.1021/acssusresmgt.4c00282
ACS Sustainable Resour. Manage. XXXX, XXX, XXX−XXX